Energy Conversion and Management 209 (2020) 112660

Contents lists available at ScienceDirect

Energy Conversion and Management

journal homepage: www.elsevier.com/locate/enconman

Boosted mutation-based Harris hawks optimizer for parameters identification of single-diode solar cell models

Hussein Mohammed Ridha[a], Ali Asghar Heidari[b,c], Mingjing Wang[d], Huiling Chen[e,*]

[a] Department of Electrical and Electronics Engineering, Faculty of Engineering, Universiti Putra Malaysia, 43400 Serdang, Malaysia
[b] School of Surveying and Geospatial Engineering, College of Engineering, University of Tehran, Tehran, Iran
[c] Department of Computer Science, School of Computing, National University of Singapore, Singapore, Singapore
[d] Institute of Research and Development, Duy Tan University, Da Nang 550000, Viet Nam
[e] Department of Computer Science and Artificial Intelligence, Wenzhou University, Wenzhou 325035, China

ARTICLE INFO

Keywords:
Photovoltaic module
Parameter extraction
Single-diode model
Harris hawks optimization
I–V characteristics

ABSTRACT

In order to realize the performance of the PV model before being installed, it is often indispensable to develop reliable and accurate parameter identification methods for dealing with the PV models. Up to now, several stochastic methods have been proposed to analyze the feature space of this problem. However, some of the stochastic-based methods may present unsatisfactory results due to their insufficient exploration and exploitation inclinations, and the multimodal and nonlinearity existed in PV parameters extraction problems. In this paper, a Boosted Harris Hawk's Optimization (BHHO) technique is proposed to achieve a more stable model and effectively estimate the parameters of the single diode PV model. The BHHO method combines random exploratory steps of evolution inspired by the flower pollination algorithm (FPA) and a powerful mutation scheme of the differential evolution (DE) with 2-Opt algorithms. The proposed strategies not only help BHHO algorithm to accelerate the convergence rate but also assist it in scanning new regions of the search basins. The results demonstrate that the proposed BHHO is more accurate and reliable compared to the basic version and several well-established methods. The BHHO method was rigorously validated by using real experimental data under seven sunlight and temperature conditions. Furthermore, the statistical criteria indicate that the proposed BHHO method has lower errors among other peers, which is highly useful for real-world applications.

1. Introduction

Nowadays, renewable energy sources (REs) are rapidly increasing in a way to deal with critical issues such as the depletion of conventional energy sources. There are various kinds of renewable energy sources such as solar energy, wind power, hydroelectric energy, biomass, hydrogen, and fuel cells, geothermal power, and other types of energy. Among these renewable energy sources, solar energy is fully available, and it is economically viable. It conducts sustainable, cost-effective, and eco-friendly energy sources. The photovoltaic (PV) technology is considered as one of the most exciting topics by researchers and companies to improve their energy conversion and reduce the total cost [1–3].

To enhance the PV system's performance, a satisfactory model of PV cells and modules is essential. The non-linearity and intermittent of meteorological data make the identification of the parameters of PV cells a challenging task [4]. Moreover, the manufacturers give performance warranty periods of PV modules for more than 25 years; PV arrays are location-dependent and inevitably undergone normal degradation with the possibility of occurring faults. Therefore, it is conceived to work on a model that simulates the real behaviour of PV cells at any operational conditions [5]. In general, the single, double, and three diode models are most common for PV cells. However, the single diode model is commonly utilized in the estimation of its parameters due to simplicity and accuracy. The double diode model is assumed to be more accurate, especially in a low solar irradiance, but it needs a longer time of computation [6]. In solar power generations, appropriate PV cell models are essential to be used for their application. Therefore, the estimation of the I-V curve can be categories into measuring methods: online and offline methods. However, online methods have a higher cost and long-term requests. In this way, offline methods by using dynamic models have to apply to predict the I-V curve at numerous weather conditions.

The PV parameters extraction techniques have been classified into five methods, such as numerical, analytical, metaheuristic, and hybrid

* Corresponding author.
E-mail addresses: gs46648@student.upm.edu.my (H.M. Ridha), as_heidari@ut.ac.ir, aliasghar68@gmail.com, aliasgha@comp.nus.edu.sg, t0917038@u.nus.edu (A.A. Heidari), mingjingwang@duytan.edu.vn (M. Wang), chenhuiling.jlu@gmail.com (H. Chen).

https://doi.org/10.1016/j.enconman.2020.112660
Received 1 December 2019; Received in revised form 24 February 2020; Accepted 26 February 2020

Nomenclature

d	ideality factor of diode
V_T	diode thermal voltage (V)
V	voltage conducted by PV module (V)
I_Ph	photocurrent (A)
q	charge particle
$S1-S7$	operational condition (solar radiation and cell temperature)
I	current conducted by the PV module (A)
I_o	saturation current of the diode (A)
$U_{rand}(t)$	randomly chosen between [0,1]
I_p	proposed current
I_e	experimental current
U_m	average position of hawk
F	scaling factor
$U(t+1)$	position vector for next generation
$U_{prey}(t)$	position of the prey
q, r_1, r_2, r_3, andr_4	randomly chosen within interval (0,1)
Y	dimension of the problem
ϵ	uniform distribution with interval (0,1)
LF	levy flight
UB	upper bounds of variables
LB	lower bounds of variables
STC	standard test condition
SD	standard deviation of RMSE
TC	cell-temperature
kB	Boltzmann constant (1.380603e-23 J/K)
AE	absolute error
RMSE	root mean square error
MBE	mean bias error
EE	energy of a prey
$U_j(t)\&U_k(t)$	Pollen from various flowers
R^2	determination coefficient
β^t	randomly distributed between (0,1)
R_s	shunt resistance(Ω)
R_p	series resistance (Ω)
FA	firefly algorithm
IADE	Improved adaptive DE.
MFA	moth-flame optimization
NR	Newton Raphson
PDE	penalty based differential evolution
ER-WCA	evaporation rate water cycle algorithm
SSA	salp swarm optimization
CPU	central processing unit
BHHO	Boosted Harris hawk's optimization
PSO	particle swarm optimization
DE	differential evolution
ABC	artificial bee colony
FPA	flower pollination algorithm
IEM	improved electromagnetism-like algorithm

[7,8]. The numerical methods have been widely used to identify the parameters of single-diode and double diode PV models with the efforts of enhancing their convergence to the optimum solution and reliability. Some examples are the least squares (Newton model) [9], Levenberg Marquardt [10], piecewise the I-V curve-fitting method [11], and other numerical methods [5]. The numerical method tends to be accurate when there is an extended data point of the I-V curve for this purpose. Moreover, the accuracy of the numerical method based on the mean absolute percentage error (MAPE) is about (90.5–99%). However, the main drawback is that the estimated parameters are susceptible to the initial conditions, which can be trapped into local minima. In addition to that, the numerical takes a long execution time than other methods. The analytical method is most widely utilized techniques that attempts to find mathematical relationship between critical points, such as short-circuit point (SC), open-circuit (OC) point, and maximum power point (MPP), and extracted parameters of PV model under standard test conditions (STCs) and different weather conditions [6,12]. The advantage of the analytical method is fast and straightforward, which uses the three key points provided by the manufactures or measured site, and then, the derivative equations of the critical points are solved to obtain the parameters of PV models [13,14]. However, the explicit analytic models do not consider the non-linear functions and transcendental of the PV models. Moreover, the accuracy of the critical points-based methods is based on the insufficient information given by the manufactures. Finally, the provided parameters values of PV panels vary from one manufacturer to another, which describes ideality behavior solely at STC [15,16]. Therefore, a remarkable percentage error between the actual and simulated performance of the PV models can be produced [17].

The stochastic methods can be further categorized into heuristic and metaheuristic methods that have been employed to tackle the shortcomings of the previous methods, such as initial conditions and long execution time [18–26]. Moreover, the stochastic methods show better performance than numerical and analytical methods in terms of convergence speed, reliability, and accuracy [8]. Mathematical models with an exact logical process can also be used for any problem in engineering [27–34]. However, some of these methods could easily fall in local minima, and the difficulty of setting control parameters are the main disadvantages of the stochastic methods. The accuracy of stochastic methods based on MAPE is about (78–98.6%). Therefore, several researchers inspired the rules of nature to develop stochastic methods such as artificial neural network (ANN) [35,36], particle swarm optimization (PSO) [37], artificial bee colony (ABC) [38], differential evolution (DE) such as PDE [39], IADE [40], and RC-IJADE [41], salp swarm algorithm (SSA) proposed by Mirjalili et al. [42], butterfly optimization algorithm (BOA) proposed by Arora et al. [43], cuckoo search (CS) [44], firefly algorithm (FA) [45–47], flower pollination algorithm (FPA) [48], electromagnetism-like EM algorithm proposed by Birbil et al. [49], moth-flame optimization (MFO) [50], whale optimization algorithm (WOA) [51], multi-verse optimizer (MVO) [52], evaporation rate water cycle algorithm (ER-WCA) [53], and Harris hawks optimization (HHO). A summary of the benefits and detriments of various stochastic methods is tabulated in Table 1.

Stochastic methods have widely used to solve complex and multimodal such as PV parameters extraction problems. However, some of these methods have limitations in terms of the exploration and exploitation phases. In the exploration phase, the algorithm utilizes its operators randomly to explore new areas and sides of the search space. Hence, exploratory behaviors have efficiently employed to allocate randomly more solutions. Meanwhile, the exploitation phase is usually performed after the exploration stage. The algorithm tries to find better solutions within the neighborhood areas and inside the search space. Therefore, a good tradeoff between the exploration (diversification) and exploitation (intensification) tendencies is an important target for the estimation of PV parameters. Since the variables (a, R_s, R_p, I_{ph}, I_o) of the single-diode PV model are individually vary from one to another case, the optimizers may trap into local optima. Several of stochastic methods present unsatisfactory performance in finding global solutions over nonlinear and multimodal objective functions [54]. Thus, achieving a more steady balance between exploration and exploitation is still a bit challenging task. It helps to avoid trapping in local minima and premature convergence.

On the other hand, hybrid evolutionary methods have widely carried out by scholars and researchers to realize different real-world cases

Table 1
Advantages and disadvantages of stochastic methods.

Approach	Advantage	Disadvantage
ANN [35,36]	• It requires less formal statistical training. • The ability for multiple training algorithms. • It is prone to overfit. • The development of ANN is empirical.	• It is considered as a black box, which needs an extensive input I-V curve data. • It is represented as complex location depended
PSO [37]	• Fast convergence speed. • It has a simple calculation. • Has a character memory.	• Easily fall into local minima. • Difficulty in finding appropriate inertia weights values.
DE [39–41]	• Improve the capacity of the search space. • It can find the optimum minimum of a multi-model search space. • It has a robust mutation scheme.	• DE has two sensitive parameters, which are scaling factor (F), and crossover (CR). They required to be tuned carefully.
ABC [38]	• Few setting parameters. • High flexibility and fast convergence. • It can avoid the effect of noise conditions.	• Premature convergence at the end of the search period. • It is not able to find optimal values sometimes. • Improbable randomly selected of scout bee reduces the accuracy of the algorithm.
(CS) [44]	• Improvement in search strategy by using Levy flights.	• Slow convergence speed to optimal values. • Walk random nature leads the CS to out-of-bounds parameters.
SSA	• Simplicity and flexibility as it is inspired by real-world behavior.	• Slow convergence speed. • It gets stuck in local optimal.
BOA	• Powerfully and exploration ability.	• Dropping into some local minima. • It has less sensitivity to stimulus changes in search space. • Lack of exploitation to optimal values.
FA [45,46]	• Has the ability to deal with a multimodal and nonlinear optimization problem. • Uses local attraction to influence the behavior of the search space.	• It is assumed to be computationally extensive for objective evaluations. • The intensity of the light is decreased with distance from its source. • If the diversity of the population is low, FA can easily trap into local minima.
FPA [48]	• Simple, efficient, and few particles are required to be tuned. • Biotic and abiotic pollinations were used to simulate global and local searches.	• The probability switch (P) should properly be controlled to solve the optimization problem. • Has weak convergence when it deals with continues domain problems.
EM	• It has a good exploration ability. • Capable of working on complex optimization problems.	• The exploitation process is limited due to the electromagnetic rules acting on the particles. • The local search and total force calculations step takes a large execution time compared with other stochastic methods.
MFO [50]	• Uses adaptive convergence constant (r) to accelerate convergence rate. • A small number of parameters are required. • It uses a higher execution time.	• Using the same angle to the light source could reduce the exploration process. • In some cases, the constant parameter (r) prevents from finding the global optimum.
WOA	• Good in the exploration phase. • Various feature selection techniques were utilized to move forward to the best solution.	• Limited in search mechanism exploitation phase. • Premature convergence.
MVO	• White and black holes were used to emphasize the exploration phase. • TDR was obtained to increase the exploitation phase. • Fast convergence rate.	• In some high multi-dimensional model falling to get global minima.
ER-WCA [53]	• Evaporation and raining processes were utilized to avoid getting trapped in local minima. • Has exploitation tendency.	• Local minima may still occur on multimodal optimization problem. • Restricted exploration process due to the stochastically explored of the search space.
HHO	• Uses surprise pounce strategy by considering several exploratory and exploitative phases. • Escaping energy is employed to make synchronization between exploration and exploitation to prevent trapping into local minima.	• Many randomly scaling coefficients have been used which leads to jumping optimal solutions regions. • Some of the utilized strategies may not present satisfactory performance for higher multimodal dimensions problems. • Escaping energy may change convergence rapidly to the optimal solutions which may be trapped into local minima.

[55–60]. One of the main problems is to estimate the parameters of PV cells. The reason for that, the hybrid methods can tackle the limitation of the previous methods such as big dimensional problems, avoiding trapping in local optima, and some of them can reduce execution time. Moreover, the accuracy of the hybrid methods based on MAPE is about (87.4–92%), which has the best accuracy compared with other methods [61–67]. However, complexity is the main obstacle to these methods. Last but not least, hybrids methods can discover various regions of the search space and allow a decision-maker to consider the quality of solutions from multiple solutions [68]. However, it has been scientifically by the well-known No-Free-Lunch (NFL) theorem [69]. Based on that, there is much room for evolving current algorithms to find better solutions for specific problems.

Recently, Rabeh et al. [62] have been employed as a hybrid method by combining analytical and SSA methods to identify the parameters of DD PV panels. The parameters I_{ph}, I_{01}, I_{o2}, R_s, R_p are analytically computed at STC. Then, the variables of the double-diode PV model are extracted by using SSA with obtaining the mean square error as an objective function to be minimized. The outdoor measurements, at various weather conditions, were applied in this study. The performance results showed the superiority of SSA compared with the gravitational search algorithm (GSA), sine cosine algorithm (SCA), WOA, ant lion optimizer (ALO), and virus colony search (VCS) in terms of accuracy. In meanwhile, the authors of [61], proposed a biogeography-based heterogeneous cuckoo search (BHCS) algorithm to extract the parameters of various PV models. Two strategies were used to achieve a better balance between exploration and exploitation phases, where the CS algorithm with using levy flight (LF) concept and quantum mechanism were employed for the exploration phase. In contrast, a biogeography-based discovery operator was utilized for the exploitation phase. Besides, the authors of Ref. [70] developed an enhanced HHO algorithm, referred to as (EHHO), by integrated the opposition-based learning (OBL) mechanism and chaotic local search (CLS) strategy to identify the parameters of PV solar cells and modules. The OBL mechanism was used to explore the feature space. Also, the CLS strategy was employed to exploit the neighborhood of solutions. The results of

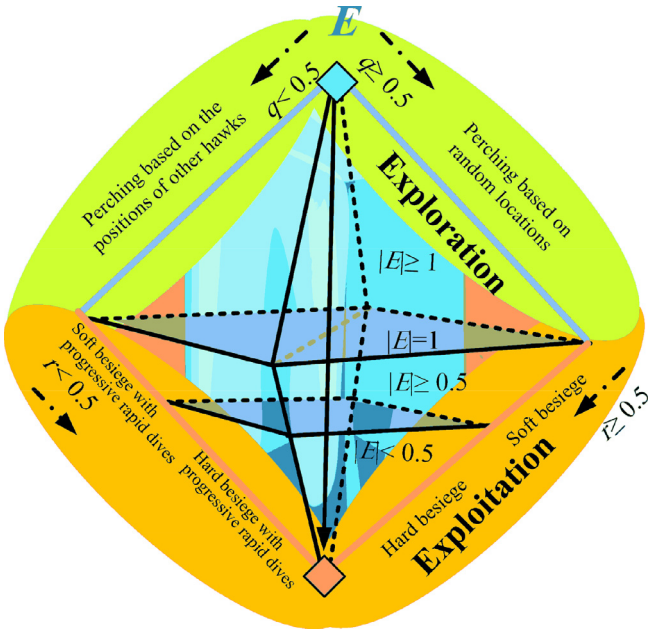

Fig. 1. The main stages of HHO can be interpreted by a logical diagram.

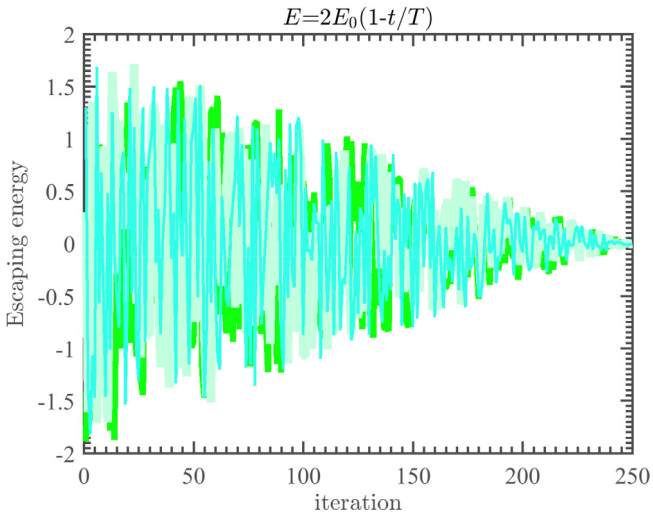

Fig. 2. The behavior of two intervals escaping energy.

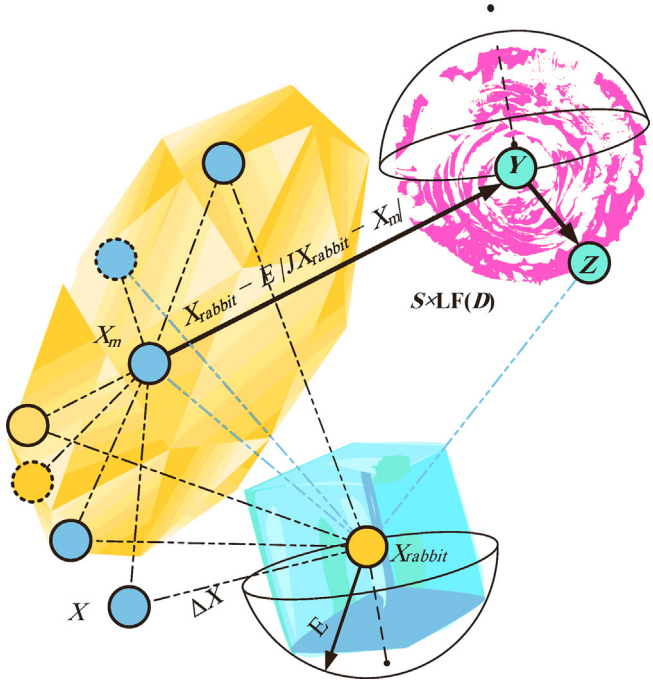

Fig. 3. A conceptual illustration of the hard besiege with progressive dives.

the EHHO method expressed the superiority over other methods mentioned in the literature. Ridha et al. proposed an improved electromagnetism-like (IEM) algorithm to estimate the five parameters of a single-diode PV module's model [71]. In IEM, a nonlinear equation was introduced to adjust the length of the particle in each iteration, and the total force formula is simplified to speed up the exploration for an optimal solution. In [72], an improved sine cosine (ISCA) method is conducted to determine the unknown parameters of the SD and DD PV cells as well as PV modules. The contribution of the authors in [72] was performed by combining Nelder-Mead simplex (NMs) and the opposition-based learning (OBL) algorithms to achieve better performance between exploration and exportation phases. The final results demonstrated that the ISCA has minimum RMSE values compared with recently published methods.

The main contributions of this research study are given by the following:

- A BHHO method is developed to identify the parameters extraction of the single-diode model using real experimental data at various environmental conditions.
- The ability of Escaping Energy (EE) is enhanced by using two different intervals to enable a more strong searching direction.
- The diversity of the population is improved by replacing it with random steps inspired by FPA using the LF concept.
- Moreover, the effective mutation scheme of the DE approach integrated with the 2-Opt algorithm is used to speed up the convergence rate and find a better solution for replacing with the worst one.
- An adapting scaling factor (F) in mutation in each iteration can balance between exploration and exploitation phases.
- Several statistical criteria are used to validate the performance results of the proposed BHHO algorithm.

Finally, comparison results indicated that the BHHO algorithm has higher accuracy and more stability among the compared well-published algorithms.

2. Photovoltaic models

According to the literature, different mathematical models have been utilized for establishing the I-V curve characteristics of solar cells and PV modules. In general, two models have been popularly utilized: the single-diode model and the double-diode model. The double-diode model is preferred at low irradiance levels due to its high accuracy [7,73,74]. However, the double-diode model is more complex and takes longer execution time compared to the single diode model. Thus, the single-diode model is widely considered for the prediction of the output current due to its simplicity and accuracy. In this section, the representation of the single-diode model and its objective function will be introduced.

2.1. Single-diode model

The circuit comprises a current source I_{Ph} in parallel, which has a high sensitivity to the meteorological data, a diode in the opposite form to be utilized for the representation of the output voltage of the PV solar cell, and two resistors. The large shunt resistance represents the saturation current of the diode, and series small resistance denotes the

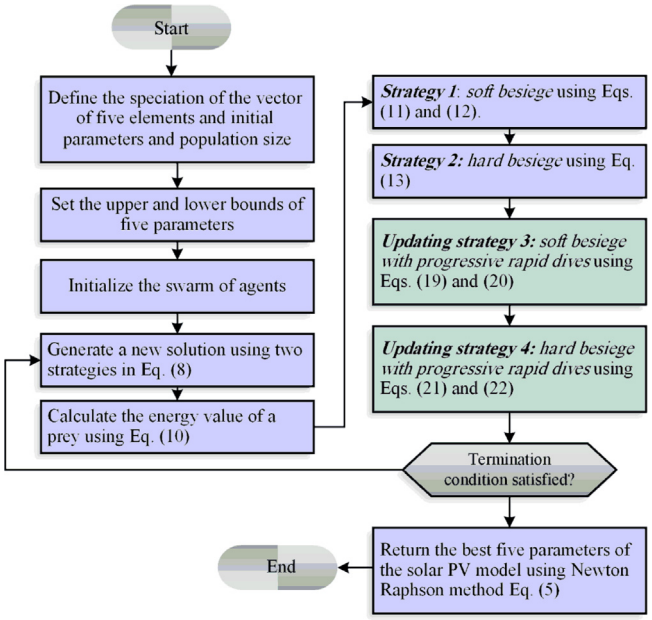

Fig. 4. Flowchart of the PV parameter extraction process using the BHHO algorithm.

Table 2
A Kyocera KC120-1 PV module specification.

Characteristics	Value
Maximum power at STC (P_{max}) in (W_P)	120
Open-circuit voltage (V_{OC}) in (V)	21.5
Short-circuit current (I_{SC}) in (A)	7.45
Voltage at MPP (V_{mp}) in (V)	16.9
Current at MPP (I_{mp}) in (A)	7.1
Nominal Operation Cell Temperature (NOCT) in (°C)	43.6
Number of cells connected in series	36
Temperature coefficient of I_{SC} (α) in (mA/K)	1.325
Temperature coefficient of V_{SC} (β) in (mV/K)	−77.5

internal loss of a solar cell. The output current can be calculated using Kirchhoff's current law as follows:

$$I = I_{Ph} - I_d - I_p \tag{1}$$

where I refers to the output current, I_d denotes to the diode current, and I_p represents the shunt resistor current. In meanwhile, I_d is calculated according to the Shockley diode equation as the following:

$$I_d = I_o\left[exp\left(\frac{V + IR_s}{V_t}\right) - 1\right] \tag{2}$$

where I_o denotes the diode reverse saturation currents related to the diode (in A), V is the output voltage, R_s refers to the series resistance, V_t represents the diode thermal voltage (in V), which is:

$$V_t = \frac{dKBT_c}{q} \tag{3}$$

where d is the diode ideality factor which refers to the diffusion current's components., T_c represents the cell temperature (K), kB is the Boltzmann constant ($1.3806503exp-23J/K$), and q refers to the electron charge ($1.60217646exp-19\ C$).

The shunt resistor current I_p is calculated as follows:

$$I_p = \frac{V + IR_s}{R_p} \tag{4}$$

where R_p denotes to the shunt resistance. Hence, by combining Eqs. (1)–(4), the output current can be given in Eq. (5).

$$I = I_{Ph} - I_o\left[exp\left(\frac{V + IR_s}{V_t}\right) - 1\right] - \frac{V + IR_s}{R_p} \tag{5}$$

There are five unknown parameters (I_{Ph}, I_o, R_s, R_p and d) is required to be extracted in the single-diode model. Thus, these five parameters can be identified by using an optimization technique to reflect the actual performance of the solar cell.

2.2. Objective function

In order to reduce the variation between the experimental and simulated data, the five parameters of the PV cell must be converted into an optimization problem. Therefore, the curve fitting values of a single-diode PV-module are evaluated at various points in the I–V curve. The objective function is represented in the form of root mean square error, and it is expressed in Eqs. (6) and (7).

$$RMSE = \sqrt{1/N\sum_{i=1}^{N} P(V_e,I_e,\theta)^2} \tag{6}$$

where

$$P(V_e,I_e,\theta) = I_e - I_{ph} + I_o\left[\exp\left(\frac{V_e + IR_s}{V_t}\right) - 1\right] + \left(\frac{V_e + IR_s}{R_p}\right) \tag{7}$$

whereI_e and V_e represent the values of the experimental current and voltage of the PV model, respectively. θ refers to the vector of the five parameters, while N denotes the data length of the I–V curve.

3. Harris hawks optimization

HHO is a novel nature-inspired proposed by Heidari et al. [75]. HHO has been improved and widely utilized to different real-world optimization problems such as image de-noising for obtaining the optimized parameters of thresholding function [76]. In addition, the HHO method was successfully applied to solve the load dispatch optimization problem in the power system in [77]. The HHO algorithm is a *meta*-heuristic population-based approach that tries to inspire the behaviour and chasing style of Harris hawks in nature, which is known as surprise pounce. HHO employs several intelligence strategies to attack prey in various ways and make the prey astonished [78]. Different chasing styles, including switching activity, are demonstrated by Harris' hawks inspired by the dynamic nature of circumstances and the prey's escaping patterns. In this process, the leader (best hawk) stoops at the prey and keeps an eye on it for a while; then, the chase will be replaced by another hawk. The switching activity is applied in different situations in order to confuse the quarry, which can increase the probability of its capturing. Based on that, there are some phases in HHO that is expressed in the next subsections. Fig. 1 also demonstrates the conceptualization of this method.

Table 3
Data points of the experimental (I-V) curve for different operational conditions [85].

Environmental condition	S1	S2	S3	S4	S5	S6	S7
Length of data points (N)	22	24	50	91	92	101	102
Solar irradiance (W/m^2)	118.28	148	306	711	780	840	978
Cell temperature (K)	318.32	321.25	327.7	324.21	329.1	331.42	328.56

Table 4
The results of the extracted parameters of the SD PV module by different algorithms.

Parameters	Method	S1	S2	S3	S4	S5	S6	S7
	BHHO	1.1235	1.2142	1.0306	1.3000	1.0592	1.3489	1.3542
	HHO	1.4590	1.3755	1.0885	1.1503	1.1042	1.3497	1.3752
	WOA	1.4106	1.2534	1.2773	1.4266	1.1421	1.3202	1.3740
	FPA	1.4428	1.4013	1.3823	1.3429	1.3666	1.3223	1.3139
	FA	1.2402	1.2906	1.1023	1.2338	1.3208	1.3491	2.3762
	ER-WCA	1.4446	1.4114	1.2980	1.3420	1.3824	1.3469	1.3760
	MVO	1.3819	1.3536	1.3899	1.1968	1.3821	1.3406	1.3710
d	MFO	1.5304	1.4852	1.3032	1.4151	1.3822	1.2045	1.3747
	SSA	1.4832	1.4094	1.3357	1.3321	1.372	1.2794	1.3595
	BOA	1.2706	2.0000	1.4526	1.4222	1.2386	1.3516	2.0000
	ABC	1.5256	1.3337	1.1942	1.3750	1.4591	1.5290	1.4352
	CS	1.5190	1.2822	1.3546	1.2821	1.2742	1.2064	1.3742
	EM	1.2651	1.4577	1.3572	1.2801	1.2441	1.3000	1.1687
	Rcr-IJADE	1.3151	1.3954	1.2652	1.3814	1.3566	1.3438	1.3600
	IADE	1.1679	1.3420	1.2442	1.3186	1.3708	1.3490	1.3740
	PDE	1.1970	1.2796	1.1757	1.2893	1.3259	1.3491	1.3762
	PSO	1.1961	1.5021	1.2376	1.4489	1.2783	1.7107	1.7126
	BHHO	0.8427	1.0228	1.9321	4.4170	5.2119	5.1522	6.3396
	HHO	0.8589	0.9017	1.924	4.3672	4.89600	5.1388	6.1563
	WOA	0.8552	0.9789	1.9743	4.4202	4.9538	5.2933	6.2718
	FPA	0.8586	0.9120	1.9402	4.3281	4.9927	5.2220	6.1654
	FA	0.8391	0.9015	1.9520	4.4214	5.154	5.5493	6.4917
	ER-WCA	0.8495	0.9100	1.9426	4.4066	5.1444	5.2778	6.4914
	MVO	0.8714	0.9074	1.9541	4.3512	5.1698	5.2003	6.2754
I_{Ph}	MFO	0.8549	0.9146	1.9459	4.3951	5.1191	5.5369	6.1546
	SSA	0.8242	0.9687	1.8601	4.5363	5.0423	5.1419	5.1602
	BOA	1.1787	0.5000	1.7307	5.1127	5.6988	7.0774	8.0000
	ABC	0.7302	0.8395	1.7870	5.3362	5.1912	5.8460	7.1073
	CS	0.8644	0.8690	2.0659	4.4469	4.7972	5.2680	6.4618
	EM	0.8411	0.9125	1.9521	4.4088	4.9138	5.2732	6.4046
	Rcr-IJADE	0.8403	0.9085	1.9478	4.4052	5.0485	5.3180	6.2239
	IADE	0.8389	0.9006	1.9395	4.4076	5.1507	5.5439	6.5018
	PDE	0.8344	0.9016	1.9416	4.4163	5.1537	5.5489	6.4921
	PSO	0.9231	0.9311	1.8808	4.5061	4.9286	6.5989	6.5543
	BHHO	1.36E-07	6.29E-07	1.03E-07	3.09E-06	1.76E-07	9.96E-06	8.13E-06
	HHO	4.87E-06	3.56E-06	2.56E-07	4.73E-07	3.59E-07	1.00E-05	1.00E-05
	WOA	3.42E-06	9.61E-07	2.61E-06	7.34E-06	6.23E-07	7.67E-06	9.54E-06
	FPA	4.38E-06	4.39E-06	7.50E-06	4.86E-06	8.69E-06	7.36E-06	5.21E-06
	FA	5.99E-07	1.52E-06	3.05E-07	1.43E-06	5.38E-06	1.00E-05	1.00E-05
	ER-WCA	4.51E-06	4.80E-06	3.32E-06	4.86E-06	1.00E-05	1.00E-05	9.99E-06
	MVO	2.51E-06	2.89E-06	8.23E-06	9.02E-07	9.37E-06	9.02E-06	8.80E-06
I_o	MFO	9.00E-06	8.84E-06	3.49E-06	1.00-E5	1.00-E5	2.03E-06	1.00E-05
	SSA	6.28E-06	4.49E-06	5.06E-06	3.66E-06	8.41E-06	4.82E-06	8.47E-06
	BOA	1.70E-06	1.00E-05	8.31E-06	2.17E-06	3.15E-06	6.58E-06	1.00E-05
	ABC	7.16E-06	2.33E-06	1.06E-06	9.34E-06	7.90E-06	3.98E-06	6.52E-06
	CS	8.51E-06	1.38E-06	6.19E-06	2.98E-06	3.58E-06	2.24E-06	1.00E-05
	EM	7.95E-07	7.08E-06	5.94E-06	2.47E-06	2.34E-06	6.18E-06	9.11E-07
	Rcr-IJADE	1.34E-06	4.15E-06	2.33E-06	7.20E-06	7.84E-06	9.36E-06	8.71E-06
	IADE	2.47E-07	2.54E-06	1.84E-06	3.80E-06	8.94E-06	9.99E-06	9.69E-06
	PDE	3.57E-07	1.35E-06	8.15E-07	2.75E-06	5.68E-06	9.99E-06	9.99E-06
	PSO	3.13E-07	1.00E-05	1.80E-06	5.37E-06	3.49E-06	8.31E-06	8.10E-06
	BHHO	1.7279	0.3937	0.7914	0.5240	0.3456	0.2006	0.1851
	HHO	1.5151	0.3124	0.7701	0.5961	0.3887	0.1999	0.2303
	WOA	1.2067	1.2467	0.7691	0.7834	0.3888	0.2296	0.2670
	FPA	1.3569	0.4334	0.5229	0.5014	0.3194	0.2456	0.2592
	FA	1.5951	0.5595	0.7540	0.5421	0.2624	0.1828	0.1811
	ER-WCA	1.2736	0.3981	0.6259	0.5067	0.2452	0.2237	0.1812
	MVO	1.6569	0.4149	0.5290	0.564	0.3430	0.2288	0.2905
R_s	MFO	1.1493	0.2952	0.6336	0.4835	0.2480	0.2281	0.2282
	SSA	0.7099	1.1961	0.3028	0.6926	0.3785	0.2261	0.2400
	BOA	0.5675	2.0000	0.4401	1.7296	0.5569	0.8774	2.0000
	ABC	0.5307	0.4155	0.8561	0.7000	0.9133	1.4498	0.5694
	CS	0.8023	0.3088	0.4873	0.4515	0.3074	0.2929	0.2744
	EM	1.5475	0.3316	0.5935	0.5298	0.3290	0.2373	0.2555
	Rcr-IJADE	1.4748	0.4272	0.6692	0.4937	0.2700	0.2314	0.2224
	IADE	1.6820	0.4906	0.6722	0.5150	0.2483	0.1831	0.1828
	PDE	1.6418	0.5805	0.7336	0.5221	0.2612	0.1829	0.1811
	PSO	0.3073	0.2069	0.4324	1.1448	0.3108	1.5742	1.5782
	BHHO	1873.90	88.34	383.49	223.43	29.77	5748.7	40.65
	HHO	5943.80	5902.97	3013.46	597.58	5342.2	7660.03	7998.83
	WOA	2544.74	365.66	5787.27	5774.68	4490.66	1004.52	730.07
	FPA	8000	6238.44	5788.69	8000	6884.75	4762.27	4753.52

(*continued on next page*)

Table 4 (*continued*)

Parameters	Method	S1	S2	S3	S4	S5	S6	S7
	FA	8000	7900.19	297.18	137.66	41.15	35.42	28.51
	ER-WCA	6475.07	8000	8000	275.13	45.13	8000	28.21
	MVO	1222.69	4379.21	3648.5	871.89	70.65	7888.47	514.8
R_p	MFO	7999.06	7999.73	7998.75	980.77	50.29	33.79	8000
	SSA	3406.93	3943.83	4062.91	2640.92	7999.39	4704.35	4509.411
	BOA	2244.63	8000	498.46	465.58	1422.79	275.21	10
	ABC	5572.27	5529.32	6840.35	789.27	1789.33	3034.26	5194.57
	CS	5880.81	8000	257.53	461.15	8000	2162.5.26	8000
	EM	6488.74	7999.83	6719.28	203.86	2756.86	1606.2	33.51
	Rcr-IJADE	6991.72	6823.8	2594.73	317.88	77.98	185.84	137.76
	IADE	1466.61	6731.9	2006.37	257.36	43.62	35.93	27.75
	PDE	6714.45	6643.67	1019.33	175.22	41.42	35.48	28.48
	PSO	86.54	578.14	1477.55	4454.55	912.33	6646.08	6440.92

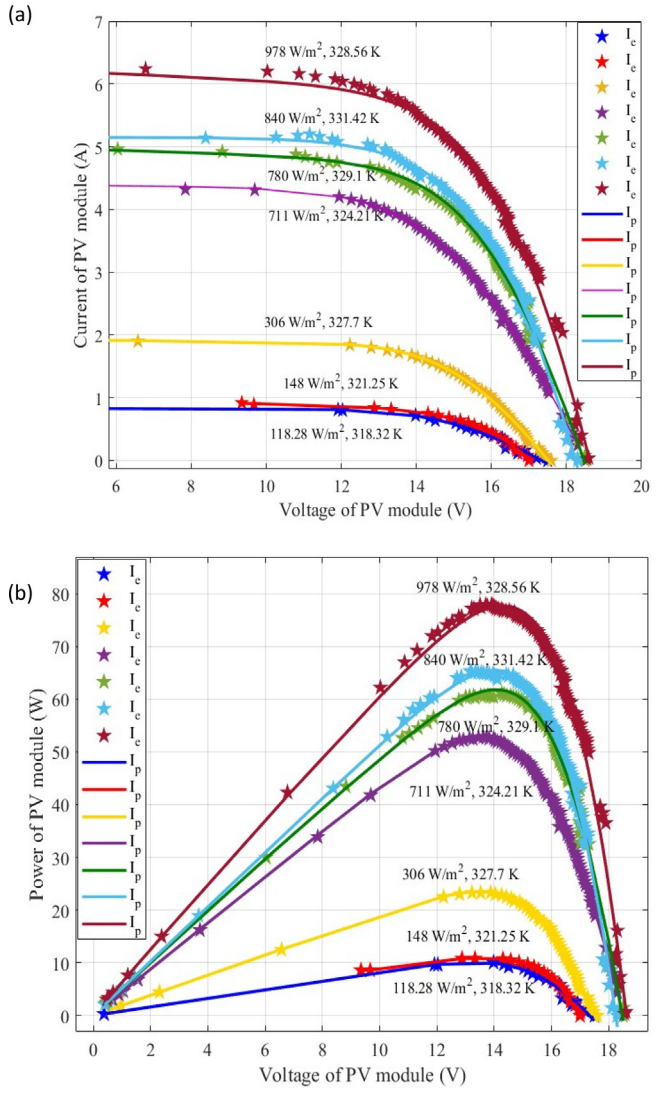

Fig. 5. PV characteristics under seven cell temperatures and solar radiations of BHHO model (a) I–V and (b) P–V curves.

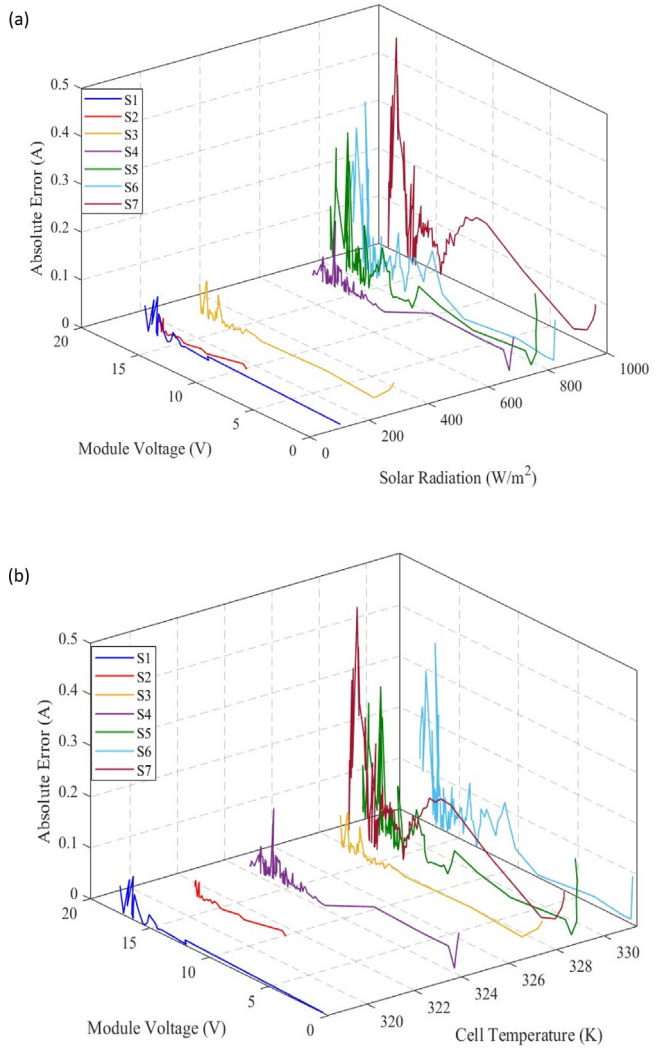

Fig. 6. The absolute errors (AE) at varying (a) solar irradiance and (b) cell temperature.

3.1. Exploration phase

Harris' hawks use two strategies to detect and chase prey randomly in some locations. This phase can be represented as follows:

$$U(t+1) = \begin{cases} U_{rand}(t) - r_1 \left| U_{rand}(t) - 2r_2 U(t) \right| & q \geq 0.5 \\ (U_{prey}(t) - U_m(t)) - r_3 (LB + r_4 (UB - LB)) & q < 0.5 \end{cases} \quad (8)$$

where $U(t+1)$ refers to the position vector of hawks in the next iteration, $U_{prey}(t)$ denotes to the position of the prey, $U_{rand}(t)$ is a randomly chosen hawk from the current population, UB, and LB are the upper and lower bounds of variables, q, r_1, r_2, r_3, and r_4 are random numbers between [0,1], and $U_m(t)$ represents the average position of hawk and can be given by the following:

Table 5
A comparison of average absolute error between BHOO and other methods.

Radiation	BHHO	HHO	WOA	FPA	FA	ER-WCA	MVO	MFO	SSA	BOA	ABC	CS	EM	Rcr-IJADE	IADE	PDE	PSO
S1	0.0231	0.0289	0.0248	0.0254	0.0291	0.0299	0.0285	0.0305	0.0274	0.1760	0.0513	0.0303	0.0292	0.0289	0.029	0.0289	0.0436
S2	0.0085	0.0093	0.0273	0.0109	0.0130	0.0139	0.0102	0.0144	0.0319	0.2208	0.0467	0.0117	0.0142	0.0137	0.0133	0.013	0.0149
S3	0.0188	0.0203	0.0321	0.0221	0.0241	0.0265	0.0215	0.0269	0.0456	0.1890	0.1485	0.0530	0.0276	0.0266	0.0262	0.0259	0.0431
S4	0.0201	0.0242	0.1395	0.0252	0.0264	0.0270	0.0220	0.0279	0.0752	0.3838	0.3172	0.0724	0.0264	0.0285	0.0265	0.0266	0.254
S5	0.0661	0.0900	0.0920	0.0815	0.0650	0.0647	0.0883	0.0648	0.0998	0.5593	0.3030	0.1493	0.0873	0.0685	0.0646	0.0649	0.0867
S6	0.0641	0.0637	0.0891	0.0685	0.0735	0.0937	0.0661	0.0801	0.0665	0.5240	0.4718	0.1433	0.0967	0.0858	0.0735	0.0735	0.7111
S7	0.1039	0.1132	0.1131	0.1169	0.0998	0.0998	0.1075	0.1155	0.1129	0.7041	0.6964	0.1728	0.1125	0.1125	0.1003	0.0998	0.5832
Average	0.0435	0.0499	0.0740	0.0501	0.0473	0.0508	0.0492	0.0514	0.0656	0.3939	0.2907	0.0904	0.0563	0.0521	0.0476	0.0475	0.2481

$$U_m(t) = \frac{1}{N}\sum_{i=1}^{N} U_i(t) \tag{9}$$

where N is the total number of hawks, and $U_i(t)$ refers to the current location of each hawk.

3.2. The transition from exploration to exploitation

During the optimization process, the energy of a prey (E) reduces during chasing and escaping behaviour, which leads the HHO algorithm to shift from exploration to exploitation phases. This can be modelled as follows:

$$E = 2E_O\left(1 - \frac{t}{T}\right) \tag{10}$$

where E_O is the energy at the first stage and can randomly be chosen inside the interval $(-1,1)$, E refers to the escaping energy of the prey, T is the number of maximum iterations. When $|E| \geq 1$, the exploration phase occurs and when $|E| < 1$, the exploitation phase happens. To emphasis the exploration and exploitation phases, the second E energy is assumed to be within the interval $(-2,2)$. The time-dependent of the E is depicted in Fig. 2.

3.3. Exploitation phase

HHO algorithms employ the surprise pounce (seven skills) in this phase by confusing attacks and astonishing the prey [79]. However, the prey tries to escape from a dangerous situation. Four strategies can be well-thought-out for describing the attacking stage. In this case, we suppose r as the chance of the prey escaping probability. When ($r \geq 0.5$), the escaping of the prey is not successful and otherwise is successful.

3.3.1. Strategy 1: soft besiege

When $|E|$ and $r \geq 0.5$, the prey fails from escaping; during this time, the Harris' hawks encircle it and then, they perform the surprise pounce. This case can be modelled as follows:

$$U(t+1) = \Delta U(t) - E\,|JU_{prey}(t) - U(t)| \tag{11}$$

$$\Delta U(t) = U_{prey}(t) - U(t) \tag{12}$$

where $\Delta U(t)$ refers to the difference between the current location and the position vector of the prey, $J = 2(1 - r_5)$ is the random jump strength of the prey during the escaping situation and r_5 is selected randomly within the interval (0,1).

3.3.2. Strategy 2: hard besiege

When $|E| < 0.5$ and $r \geq 0.5$, the prey is confused and get exhausted, the harris' hawks mightily surrounded the prey and executed the surprise pounce. The following rule can express the modeling of this strategy:

$$U(t+1) = U_{prey}(t) - E\,|\Delta U(t)| \tag{13}$$

3.3.3. Strategy 3: soft besiege with progressive rapid dives

When $|E| \geq 0.5$ and $r < 0.5$, the prey can escape successfully, and it is called *leapfrog movements* [79]. In this strategy, the optimal concept levy flight (LF) is used for considering the real zigzag motion of prey [80]. Therefore, the hawks can determine their next movement by the following equation:

$$Y = U_{prey}(t) - E\,|JU_{prey}(t) - U(t)| \tag{14}$$

$$Z = Y + S * LF(D) \tag{15}$$

where D is the dimension of the problem and S is a vector randomly chosen with the size of $(1 \times D)$, J is randomly selected to in each iteration to simulate the nature of prey motion, and the levy flight (LF) function can be calculated as follows:

$$LF = \frac{u \times \sigma}{|v|^{1/\beta}},\ \sigma = \left(\frac{\Gamma(1+\beta) \times \sin\left(\frac{\pi\beta}{2}\right)}{\Gamma\left(\frac{1+\beta}{2}\right) \times \beta \times 2^{\left(\frac{\beta-1}{2}\right)}}\right)^{1/\beta} \tag{16}$$

where v and u are randomly selected within values within (0,1), β is assumed to be constant to (1.5). The updating position of hawks in this strategy can be expressed as follows:

$$U(t+1) = \begin{cases} Y if F(Y) < F(U(t)) \\ Z if F(Z) < F(U(t)) \end{cases} \tag{17}$$

3.3.4. Strategy 4: hard besiege with progressive rapid dives

When $|E| < 0.5$ and $r < 0.5$, the prey is unable to escape successfully, and hawks try to reduce the interval of their average location. This strategy can be modelled as follows:

$$U(t+1) = \begin{cases} U_{prey}(t) - E\,|JU_{rabbit}(t) - U_m(t)|\ if F(Y) < F(U(t)) \\ Y + S * LF(D) if F(Z) < F(U(t)) \end{cases} \tag{18}$$

A general concept of this phase is shown in Fig. 3.

3.4. Boosted Harris hawks optimization

In the HHO algorithm, some of the used strategies are simple and can rapidly convergence, which may lead to avoiding some of the optimal regions. Therefore, development in exploration and exploitation phases are essential to discover more optimal areas and enhance the exploitation strategy. Therefore, the updates of *strategy (3 and 4)* can be given by the following:

3.4.1. Update strategy 3

To increase the diversity of solutions of the current population rapidly, strategy *3* is replaced with steps inspired by the flower pollination process of flowering plants [81]. In this step, biotic and cross-pollination is assumed as prey (global pollination) procedure with using levy flight concept. Hence, the abiotic and self-pollination can be treated as local pollination. Inspired by flower constancy, it can be assumed as the reproduction probability, which is proportionate to the similarity of two involved flowers [82]. The updating of the *strategy 3*

Table 6
A comparison of the experimental results between BHHO and other methods.

Parameters	Method	S1	S2	S3	S4	S5	S6	S7	Average
	BHHO	0.0333	0.0128	0.0267	0.0286	0.0919	0.0885	0.1306	0.0591
	HHO	0.0367	0.0156	0.0278	0.0324	0.1183	0.0888	0.1464	0.0663
	WOA	0.0355	0.0330	0.0386	0.1657	0.1188	0.1097	0.1537	0.0936
	FPA	0.0355	0.0152	0.0317	0.0361	0.1090	0.0980	0.1526	0.0683
	FA	0.0428	0.0164	0.3360	0.0366	0.1008	0.1024	0.1363	0.0670
	ER-WCA	0.0436	0.0170	0.0361	0.0381	0.1009	0.1204	0.1363	0.0703
	MVO	0.0367	0.0136	0.0293	0.0321	0.1162	0.0927	0.1611	0.0689
RMSE	MFO	0.0440	0.0175	0.0361	0.0394	0.1011	0.1074	0.1581	0.0719
	SSA	0.0399	0.0375	0.0578	0.0916	0.1286	0.0910	0.1478	0.0849
	BOA	0.2138	0.2548	0.2208	0.4430	0.6079	0.6840	0.9805	0.4866
	ABC	0.0623	0.0497	0.1552	0.3765	0.3966	0.6857	0.7869	0.3590
	CS	0.0421	0.0184	0.0600	0.0857	0.1819	0.1812	0.1999	0.1099
	EM	0.0429	0.0173	0.0370	0.0372	0.1197	0.1232	0.1501	0.0753
	Rcr-IJADE	0.0431	0.0169	0.0356	0.0389	0.1392	0.1172	0.1522	0.0730
	IADE	0.0426	0.0166	0.0353	0.0378	0.1092	0.1024	0.1367	0.0675
	PDE	0.0427	0.0164	0.0346	0.0373	0.1085	0.1024	0.1363	0.0672
	PSO	0.0591	0.0180	0.0591	0.2977	0.1173	0.8065	0.8053	0.3090
	BHHO	0.9832	0.9978	0.9979	0.9993	0.9947	0.9955	0.9926	0.9944
	HHO	0.9795	0.9976	0.9977	0.9991	0.9913	0.9955	0.9908	0.9931
	WOA	0.9808	0.9858	0.9956	0.9775	0.9913	0.9931	0.9898	0.9877
	FPA	0.9808	0.9969	0.9970	0.9989	0.9926	0.9945	0.9900	0.9930
	FA	0.9718	0.9964	0.9966	0.9988	0.9937	0.9943	0.9920	0.9920
	ER-WCA	0.9708	0.9962	0.9961	0.9988	0.9937	0.9922	0.9920	0.9914
	MVO	0.9795	0.9975	0.9974	0.9991	0.9916	0.9951	0.9888	0.9927
R^2	MFO	0.9703	0.9960	0.9961	0.9987	0.9937	0.9937	0.9893	0.9911
	SSA	0.9758	0.9816	0.9902	0.9931	0.9898	0.9953	0.9906	0.9880
	BOA	0.3077	0.1581	0.8572	0.8396	0.7692	0.7352	0.5883	0.6079
	ABC	0.9412	0.9679	0.9294	0.8841	0.9031	0.7339	0.7348	0.8706
	CS	0.9731	0.9955	0.9894	0.9939	0.9796	0.9814	0.9828	0.9851
	EM	0.9717	0.9960	0.9959	0.9988	0.9911	0.9918	0.9903	0.9908
	Rcr-IJADE	0.9714	0.9962	0.9962	0.9987	0.9935	0.9926	0.9901	0.9919
	IADE	0.9213	0.9963	0.9963	0.9988	0.9937	0.9943	0.9920	0.9919
	PDE	0.9720	0.9964	0.9964	0.9988	0.9937	0.9943	0.9920	0.9919
	PSO	0.9470	0.9957	0.9897	0.9272	0.9915	0.7724	0.7223	0.8994
	BHHO	−0.0258	−0.0460	−0.0321	−0.0302	0.0330	0.0296	0.07175	0.0019
	HHO	−0.0295	−0.0527	−0.0384	−0.0338	0.0520	0.0225	0.0800	0.0026
	WOA	−0.0580	−0.0605	−0.0550	0.0720	0.0252	0.0161	0.0601	0.0032
	FPA	−0.0327	−0.0531	−0.0366	0.0321	0.0406	0.0297	0.0842	0.0026
	FA	−0.0241	−0.0505	−0.0333	−0.0303	0.0337	0.0353	0.0693	0.0020
	ER-WCA	−0.0267	−0.0342	−0.0322	−0.0305	0.0305	0.0500	0.0659	0.0022
	MVO	−0.0321	−0.0550	−0.0395	−0.0367	0.0473	0.0238	0.0922	0.0030
d_i	MFO	−0.0279	−0.0544	−0.0358	−0.0325	0.0291	0.0354	0.0861	0.0026
	SSA	−0.0458	−0.0482	−0.0279	0.0058	0.0427	0.0051	0.0682	0.0019
	BOA	−0.2726	−0.2316	−0.2656	−0.0433	0.1215	0.1976	0.4941	0.0830
	ABC	−0.2967	−0.3093	−0.2037	0.0175	0.0376	0.3266	0.4279	0.0861
	CS	−0.0678	−0.0914	−0.0498	−0.0241	0.0720	0.0713	0.0900	0.0057
	EM	−0.0324	−0.0580	−0.0383	−0.0381	0.0443	0.0478	0.0747	0.0028
	Rcr-IJADE	−0.0294	−0.0556	−0.0369	−0.0336	0.0313	0.0446	0.0796	0.0020
	IADE	−0.0248	−0.0508	−0.0321	−0.0296	0.0333	0.0349	0.0692	0.0020
	PDE	−0.0245	−0.0508	−0.0326	−0.0298	0.0335	0.0035	0.0691	0.0020
	PSO	−0.2498	−0.2910	−0.2499	−0.1129	−0.1916	0.4975	0.4962	0.1233
	BHHO	0.1527	0.0617	0.1871	0.2717	0.8808	0.8888	1.3244	0.5403
	HHO	0.1684	0.0650	0.1950	0.3078	1.1374	0.8923	1.4874	0.6076
	WOA	0.1632	0.1586	0.2704	1.5940	1.1419	1.1045	1.5639	0.8566
	FPA	0.1631	0.0731	0.0.2222	0.3435	1.0462	0.9855	1.5518	0.6265
	FA	0.1967	0.0789	0.2358	0.3480	0.9670	1.0299	1.3836	0.6057
	ER-WCA	0.2003	0.0817	0.2530	0.3624	0.9678	1.2129	1.3836	0.6374
	MVO	0.1686	0.0660	0.2058	0.3051	1.1169	0.9312	1.6410	0.6336
TS	MFO	0.2020	0.0839	0.2531	0.3745	0.3745	0.9695	1.0808	1.6097
	SSA	0.1833	0.1803	0.4056	0.8735	1.2371	0.9139	1.5023	0.7565
	BOA	1.0030	1.2637	1.5849	4.6884	7.3044	9.3780	50.2431	10.7808
	ABC	0.2860	0.2387	1.1001	3.8566	4.1220	9.4204	12.8169	4.4587
	CS	0.1931	0.0885	0.4212	0.8164	1.7650	1.8430	2.0511	1.0255
	EM	0.1970	0.0831	0.2591	0.3540	1.1508	1.2420	1.52655	0.6875
	Rcr-IJADE	0.1980	0.0814	0.2498	0.3698	0.9967	1.1802	1.5479	0.6606
	IADE	0.1957	0.0800	0.2478	0.3594	0.9677	1.0300	1.3878	0.6098
	PDE	0.1961	0.0787	0.2426	0.3548	0.9670	1.0299	1.3836	0.6075
	PSO	0.2715	0.0864	0.4145	2.9588	1.1273	13.6427	13.6516	4.5933

can be represented by the following:

$$Y = U(t) + LF(U_{prey}(t) - U(t)) \quad (19)$$

$$Z = U(t) + \epsilon\,(U_j(t) - U_k(t)) \quad (20)$$

where ϵ has drawn from a uniform distribution with interval (0,1),

Table 7
MSE values of proposed BHHO and compared with other algorithms.

Method	S1	S2	S3	S4	S5	S6	S7	Average
BHHO	0.0011	0.0001	0.0007	0.0008	0.0087	0.0078	0.0170	0.0052
HHO	0.0013	0.0001	0.0007	0.0010	0.0140	0.0079	0.0214	0.0066
WOA	0.0012	0.0010	0.0014	0.0274	0.0141	0.0120	0.0236	0.0115
FPA	0.0012	0.0002	0.0010	0.0013	0.0118	0.0096	0.0232	0.0069
FA	0.0018	0.0002	0.0011	0.0013	0.0101	0.0104	0.0186	0.0062
ER-WCA	0.0019	0.0002	0.0013	0.0014	0.0101	0.0144	0.0186	0.0068
MVO	0.0013	0.0001	0.0008	0.0010	0.0135	0.0085	0.0259	0.0073
MFO	0.0019	0.0003	0.0013	0.0015	0.0102	0.0115	0.0250	0.0074
SSA	0.0015	0.0014	0.0033	0.0084	0.0165	0.0082	0.0237	0.0090
BOA	0.0457	0.0649	0.0487	0.1962	0.3658	0.4679	0.9615	0.3072
ABC	0.0038	0.0024	0.0247	0.1418	0.1573	0.4701	0.6192	0.2027
CS	0.0017	0.0003	0.0036	0.0073	0.0331	0.0328	0.0399	0.0170
EM	0.0018	0.0003	0.0013	0.0013	0.0143	0.0151	0.0225	0.0081
Rcr-IJADE	0.0018	0.0002	0.0012	0.0015	0.0108	0.0137	0.0231	0.0075
IADE	0.0018	0.0002	0.0012	0.0014	0.0101	0.0104	0.0187	0.0063
PDE	0.0080	0.0002	0.0012	0.0013	0.0101	0.0104	0.0186	0.0062
PSO	0.0033	0.0003	0.0034	0.0886	0.0137	0.8944	0.6504	0.2363

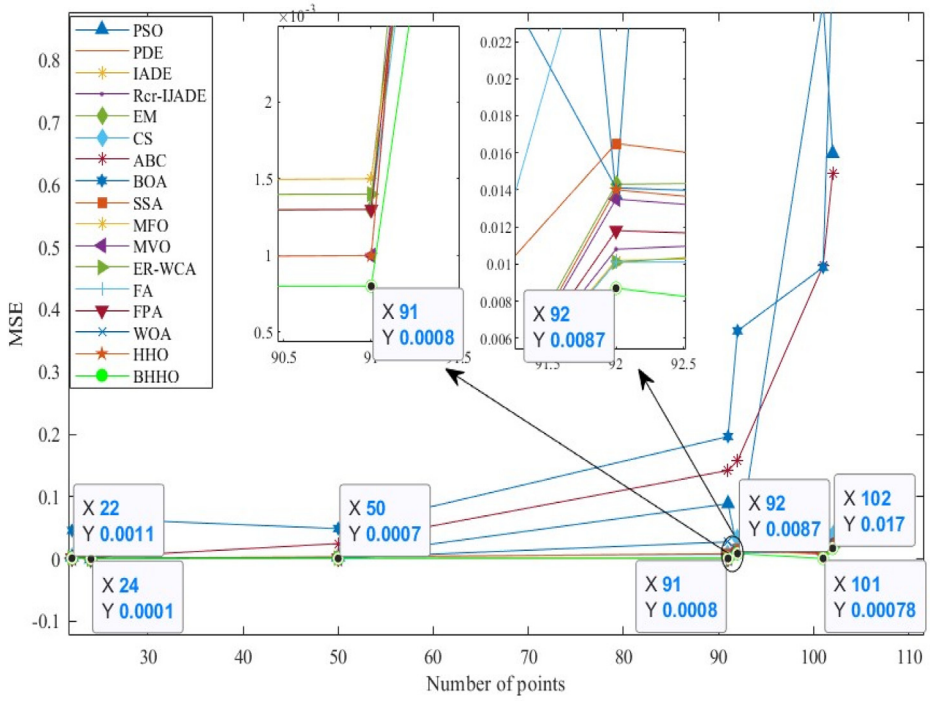

Fig. 7. MSE of BHHO and other algorithms under seven weather conditions.

$U_j(t)$and $U_k(t)$ are pollen from various flowers of the same plant species (population). Eqs. (19) and (20) are subject to the condition in Eq. (17).

3.4.2. Update strategy 4

In this strategy, the mutation of the differential evolution (DE) algorithm is obtained since DE has a powerful mutation scheme [53]. The proposed mutation vector is inspired by the 2-Opt algorithm [83]. 2-Opt algorithm was used to find routes in the traveling salesperson problem, which avoids routs from self-crossing by rescheduling them.

$$U(t+1) = \begin{cases} U_\alpha(t) + F(U_\beta(t) - U_\gamma(t)) & if\ f(U_\alpha(t)) < f(U_\beta(t)) \\ U_\beta(t) + F(U_\alpha(t) - U_\gamma(t)) & otherwise \end{cases} \quad (21)$$

where X_α^G, X_β^G, and X_γ^G are mutually distinct chosen from the population. The mutation vector in Eq. (21) not only provides a good chance to accelerate convergence rate but also it can ensure of escaping from local optima [84]. Moreover, a new scale factor (F) instead of the previous constant scale factor is used, which it can efficiency balance the local and global ability of the BHHO algorithm. It is denoted as follows:

$$F = 1.2 \times \beta^t - 1 \quad (22)$$

where β^t is a uniformly distributed number randomly within the interval [0,1]. This rule plays an important role in rising exploitation and reducing the exploration of the proposed BHHO algorithm. Fig. 4, illustrates the flowchart of the PV parameter extraction process using the BHHO algorithm.

3.5. Statistical criteria of the proposed algorithms

The following six criteria are obtained to identify the accuracy of the proposed algorithm: RMSE, coefficient of determination (R^2), standard test deviation STD, absolute error (AE), the test statistic (TS), and mean square error (MSE).

- RMSE denotes the standard deviation between experimental and proposed (I–V) curve data of a sample of N data points. This

parameter is utilized to measure unsystematic error and can be given by the following:

$$RMSE = \sqrt{\frac{1}{N}\sum_{i=1}^{N}(I_p - I_e)^2} \tag{23}$$

where N refers to data points number of I–V curve, and i represents a level of solar radiation ($i = 1, 2,\ldots, N$)

- R^2 is utilized to compute the accuracy and performance of the proposed single-diode model. This parameter reflects the difference in levels in the experimental data, which refers to a high level of consistency between the experimental and simulation results. The best value of R^2 is close to 1 and can be given by the following;

$$R^2 = 1 - \frac{\sum_{i=1}^{N}(I_p - I_e)^2}{\sum_{i=1}^{N}(I_e - \bar{I_e})^2} \tag{24}$$

where $\bar{I_e}$ represents the mean of experimental current ($\bar{I_e} = \frac{1}{N}\sum_{i=1}^{N} I_e$).

- STD, the deviation of the proposed method in the RMSE for N tests, is utilized to evaluate the proposed model results and is calculated using the following equation:

$$STD = \sqrt{\frac{1}{(N-1)}\sum_{i=1}^{N} d_i^2} \tag{25}$$

- AE is used to evaluate the absolute variation between the experimental and proposed currents for a defined voltage point at a known cell temperature and solar radiation and given by the following equation:

$$AE = |I_p - I_e| \tag{26}$$

where I_p and I_e are the proposed and experimental currents, respectively.

- TS is used to evaluate whether the estimated model is significantly different from computed data or not. The small value of TS means high accuracy of the predicted data.

$$TS = \sqrt{\frac{(N-1)MBE^2}{RMSE^2 - MBE^2}} \tag{27}$$

- MSE is the last statistical criterion that is used to measure the deviation between proposed and simulated models. The high accuracy of the proposed method indicates a small MSE value.

$$MSE = \frac{1}{N}\sum_{i=1}^{N}(I_p - I_e)^2 \tag{28}$$

4. Results and discussion

In this research study, the proposed Boosted Harris hawks optimization (BHHO)-based parameter estimation method is intensively carried out based on experimental data of a Kyocera KC120-1 multi-crystalline PV module. The adopted PV module was installed at a solar structure at the University Kembangan Malaysia, Malaysia. Data were extracted by using a DC-DC converter based on the I-V characteristics generator. The accuracy of the used I-V characteristics generator was approximately 99%–99.5% [85]. The PV specification at standard test conditions (STC) is tabulated in Table 2. The number of I-V data points for the different environmental conditions is tabulated in Table 3.

For successful implementation, the dimension of the optimization problem (dim) is set to 5 based on the five parameters of the PV model. The size of the population (N) is set to be 30. Meanwhile, the maximum number of iteration (T) is set to be 250. The value of β is set to be 1.5. The search boundaries of the single-diode PV model parameters are $d \in [0.1, 2]$, $I_{Ph} \in [0.5, 8]$, $I_o \in [1e-12.1e-5]$, $R_s \in [0.1, 2]$, and $R_p \in [0.5, 8]$ [39,40,85]. The accuracy of the proposed methods is obtained by comparing the real experimental data with the results of extracted parameters [85].

The extracted parameters of the single-diode PV model using various algorithms are shown in Table 4. The performance of all algorithms may vary with the variation of meteorological data and with consideration the effects of noise. According to the literature, the algorithms that used for comparison are PSO [37], ABC [38], PDE [39], IADE [40], and RC-IJADE [41], SSA proposed by Mirjalili et al. [42], BOA proposed by Arora et al. [43], CS [44], FA [45–47], FPA [48], EM algorithm proposed by Birbil et al. [49], MFO [50], WOA [51], MVO [52], ER-WCA [53], and HHO.

The I-V and P-V data curves for the proposed BHHO algorithm under seven weather conditions are illustrated in Fig. 5 (a) and (b). It is distinctly that the I-V and P-V curves are very close to the experimental data. However, the deviation can be observed in the near region of the maximum power point (MPP). Matching to I-V and P-V characteristics curves, the absolute error (AE) of the PV current for seven solar radiations and solar cells is depicted in Fig. 6(a) and (b). As per observations, the proposed BHHO method shows excellent accuracy for S1, S2, and S3. However, the accuracies for S4, S6, and S7 are low. The reason for that is because these levels have longer data points. The average absolute error values for the proposed BHHO method compared with various methods are given in Table 5. The proposed BHHO method has a lower average absolute error in all seven weather conditions, followed by FA, PDE, IADE, MVO, and HHO. The average absolute error values of the best six algorithms are 0.0435, 0.0473, 0.0475, 0.0476, 0.0492, and 0.0499, respectively. Whereas, the worst values of average absolute error were registered for CS, PSO, ABC, and BOA, which are 0.0904, 0.2481, 0.2907, and 0.3939, respectively.

To show the superiority of the proposed SD PV model, a comparison was performed using several statistical criteria between the BHHO approach and other algorithms in terms of RMSE, MBE, R^2, d_i, and TS, which is tabulated in Table 6. It can be noted that the FA, PDE, IADE, MVO, HHO, EM algorithms have good performance in terms of stability and average convergence. However, the proposed BHHO has lower average RMSE, R^2, d_i, STD and TS values which are 0.0591, 0.9944, 0.0019, and 0.5403, respectively. It is essential to remark that the outcomes presented in Table 6 may be the chosen best one in several runs. The WOA, CS, PSO, ABC, and BOA algorithms suffer from severer multi-modality problems due to the nonlinearly of the optimization problem and intermittent of meteorological data.

Finally, the last criterion to verify the performance of the proposed method as compared with other algorithms is MSE. Table 7 presents small MSE's values of the BHHO algorithm when compared with other algorithms. The average MSE value of the BHHO algorithm is 0.0052, which emphasizes its superiority and stability, among other algorithms. Fig. 7 indicates the MSE values of all algorithms concerning the I-V data points under various environmental conditions. From Fig. 7, we see the selected two zoomed points that clearly show the outperformance of the BHHO algorithm as well as avoiding overcrowding traces.

There are several well-evaluated reasons for the enhanced results of the proposed BHHO method compared to the other competitors. First, it utilizes the effective mutation scheme of the DE algorithm with the 2-Opt approach to accelerate the convergence tendencies of the core stages and find a better solution for replacing with the worst agent in each iteration. Also, we modified the main rule of escaping energy by using two different intervals that enable a strong searching direction. This factor significantly enriches the final internal harmony of the HHO-based variant. Also, adapting the scaling factor in mutation helps the searching trend to make a delicate equilibrium between exploration and exploitation propensities in each stage. As another reason, the diversity of the population is enriched using random steps induced by FPA with keep using the L-based jumps. This modification further helps

the proposed version to jump out of local optima and avoid situations that method cannot have progress within the next iterations (stagnation). It is also evident that the proposed BHHO preserves the chief merits of the fundamental paradigm in terms of dynamic mechanisms and high capacity of local optima avoidance. In general, the resulted version yields a more stable interchange amongst its essential searching traits. Hence, it starts the searching trends using an enhanced diversification tendency and then smoothly shifts its initial exploratory task to exploitation. At the end of iterations, the proposed mechanisms assist the version in focussing on the vicinity of high-quality agents more intensively. Therefore, it reaches to a better harmony between the diversification of agents and focusing around the better solutions (intensification trends). It is worth noting that the proposed HHO version also preserves the core time-varying dynamic traits and advantages of the basic HHO. Therefore, this BHHO method can be successfully used to describe the real behaviour of the output power energy generated by the PV module.

5. Conclusion and future directions

In this study, a Boosted Harris hawk's optimization (BHHO) algorithm has been proposed to extract the parameters of the single-diode PV module. Two strategies are adaptive for the development of the exploration and exploitation phases of the BHHO algorithm. In the first adaptive strategy, the random steps inspired by the flower pollination algorithm (FPA) with levy flight (LF) optimal concept to explore the search space. Also, an optimal mutation vector using differential evolution (DE) inspired by the 2-Opt algorithm is considered in the second adaptive strategy. Thus, the diversity of the population, rapid convergence, and global search strategies are introduced to achieve the best fit. The performance of the proposed BHHO algorithm is extensively validated using experimental data under seven weather conditions. The performance results of the proposed BHHO method exhibit a very close I-V and P-V data characteristics curves to the experimental data. Besides, the proposed method shows a high consistently converges to optimal five parameters in all environmental conditions by comparing with other methods available in the literature. The average values of RMSE, R^2, TS, AE, and MSE at seven operational conditions of the proposed method were 0.0591, 0.9944, 0.5403, 0.0435, and 0.0052, respectively.

Based on the above observed merits, the proposed BHHO method is conceived to be valuable for tacking real-optimization problems in energy fields, such as finding optimal parameters of double and three diodes PV cell/module, optimal sizing of the PV system and monitoring and fault detection of PV systems. Such directions are so exciting to be the main focus of future works.

CRediT authorship contribution statement

Hussein Mohammed Ridha: Writing - original draft, Writing - review & editing, Software, Visualization, Investigation, Formal analysis, Methodology, Conceptualization. **Ali Asghar Heidari:** Writing - original draft, Writing - review & editing, Software, Visualization, Investigation, Formal analysis, Methodology, Conceptualization. **Mingjing Wang:** Writing - review & editing, Software, Visualization. **Huiling Chen:** Conceptualization, Methodology, Formal analysis, Investigation, Writing - review & editing, Funding acquisition, Supervision.

Declaration of Competing Interest

The authors declare that they have no known competing financial interests or personal relationships that could have appeared to influence the work reported in this paper.

Acknowledgment

This research is supported by National Natural Science Foundation of China (U1809209). We acknowledge the efforts of respected editor and all anonymous reviewers for their valuable time and comments that improved the quality of this research.

References

[1] Jin T, Kim J. A comparative study of energy and carbon efficiency for emerging countries using panel stochastic frontier analysis. Sci Rep 2019:1–8. https://doi.org/10.1038/s41598-019-43178-7.
[2] Ridha HM, Gomes C, Hizam H, Ahmedipour M. Optimal design of standalone photovoltaic system based on multi-objective particle swarm optimization: a case study of Malaysia. Processes 2019:1–24. https://doi.org/10.3390/pr8010041.
[3] Mohammed Ridha Hussein, Gomes C, Hizam H, Mirjalili S. Multiple scenarios multi-objective salp swarm optimization for sizing of standalone photovoltaic system. Renew Energy 2020.
[4] Ram JP, Babu TS, Dragicevic T, Rajasekar N. A new hybrid bee pollinator flower pollination algorithm for solar PV parameter estimation. Energy Convers Manage 2017;135:463–76. https://doi.org/10.1016/j.enconman.2016.12.082.
[5] Jordehi AR. Parameter estimation of solar photovoltaic (PV) cells: A review. Renew Sustain Energy Rev 2016;61:354–71. https://doi.org/10.1016/j.rser.2016.03.049.
[6] Abbassi R, Abbassi A, Jemli M, Chebbi S. Identification of unknown parameters of solar cell models: A comprehensive overview of available approaches. Renew Sustain Energy Rev 2018;90:453–74. https://doi.org/10.1016/j.rser.2018.03.011.
[7] Chin VJ, Salam Z, Ishaque K. Cell modelling and model parameters estimation techniques for photovoltaic simulator application: A review. Appl Energy 2015;154:500–19. https://doi.org/10.1016/j.apenergy.2015.05.035.
[8] Pillai DS, Rajasekar N. Metaheuristic algorithms for PV parameter identi fi cation : A comprehensive review with an application to threshold setting for fault detection in PV systems. Renew Sustain Energy Rev 2017. https://doi.org/10.1016/j.rser.2017.10.107.
[9] Easwarakhanthan T, Bottin J, Bouhouch I, Boutrit C. Nonlinear minimization algorithm for determining the solar cell parameters with microcomputers. Int J Sol Energy 1986;4:1–12. https://doi.org/10.1080/01425918608909835.
[10] Tossa AK, Soro YM, Azoumah Y, Yamegueu D. A new approach to estimate the performance and energy productivity of photovoltaic modules in real operating conditions. Sol Energy 2014;110:543–60. https://doi.org/10.1016/j.solener.2014.09.043.
[11] Bai J, Liu S, Hao Y, Zhang Z, Jiang M, Zhang Y. Development of a new compound method to extract the five parameters of PV modules. Energy Convers Manage 2014;79:294–303. https://doi.org/10.1016/j.enconman.2013.12.041.
[12] Batzelis EI, Papathanassiou SA. A method for the analytical extraction of the single-diode PV model parameters. IEEE Trans Sustain Energy 2016;7:504–12. https://doi.org/10.1109/TSTE.2015.2503435.
[13] Dehghanzadeh A, Farahani G, Maboodi M. A novel approximate explicit double-diode model of solar cells for use in simulation studies. Renew Energy 2017;103:468–77. https://doi.org/10.1016/j.renene.2016.11.051.
[14] Elbaset AA, Ali H, Abd-El Sattar M. Novel seven-parameter model for photovoltaic modules. Sol Energy Mater Sol Cells 2014;130:442–55. https://doi.org/10.1016/j.solmat.2014.07.016.
[15] Chin VJ, Salam Z. A new three-point-based approach for the parameter extraction of photovoltaic cells. Appl Energy 2019;237:519–33. https://doi.org/10.1016/j.apenergy.2019.01.009.
[16] Soto W De, Klein SA, Beckman WA. Improvement and validation of a model for photovoltaic array performance 2006; 80:78–88. doi:10.1016/j.solener.2005.06.010.
[17] Wu L, Chen Z, Long C, Cheng S, Lin P, Chen Y, et al. Parameter extraction of photovoltaic models from measured I-V characteristics curves using a hybrid trust-region reflective algorithm. Appl Energy 2018;232:36–53. https://doi.org/10.1016/j.apenergy.2018.09.161.
[18] Ma J, Bi Z, Ting TO, Hao S, Hao W. Comparative performance on photovoltaic model parameter identification via bio-inspired algorithms. Sol Energy 2016;132:606–16. https://doi.org/10.1016/j.solener.2016.03.033.
[19] Qiao W, Huang K, Azimi M, Han S. A novel hybrid prediction model for hourly gas consumption in supply side based on improved whale optimization algorithm and relevance vector machine. IEEE Access 2019;7:88218–30. https://doi.org/10.1109/ACCESS.2019.2918156.
[20] Qiao W, Lu H, Zhou G, Azimi M, Yang Q, Tian W. A hybrid algorithm for carbon dioxide emissions forecasting based on improved lion swarm optimizer. J Clean Prod 2020;244:118612https://doi.org/10.1016/j.jclepro.2019.118612.
[21] Qiao W, Tian W, Tian Y, Yang Q, Wang Y, Zhang J. The forecasting of PM2.5 using a hybrid model based on wavelet transform and an improved deep learning algorithm. IEEE Access 2019;7:142814–25. https://doi.org/10.1109/ACCESS.2019.2944755.
[22] Qiao W, Yang Z. An improved dolphin swarm algorithm based on Kernel Fuzzy C-means in the application of solving the optimal problems of large-scale function. 1 1 IEEE Access 2019;10.1109/ACCESS.2019.2958456. https://doi.org/10.1109/ACCESS.2019.2958456.
[23] Qiao W, Yang Z. Modified dolphin swarm algorithm based on chaotic maps for solving high-dimensional function optimization problems. IEEE Access 2019;7:110472–86. https://doi.org/10.1109/ACCESS.2019.2931910.

[24] Qiao W, Yang Z. Solving large-scale function optimization problem by using a new metaheuristic algorithm based on quantum dolphin swarm algorithm. IEEE Access 2019;7:138972–89. https://doi.org/10.1109/ACCESS.2019.2942169.

[25] Qiao W, Yang Z. Forecast the electricity price of U.S. using a wavelet transform-based hybrid model. Energy 2020;193:116704https://doi.org/10.1016/j.energy.2019.116704.

[26] Qiao W, Yang Z, Kang Z, Pan Z. Short-term natural gas consumption prediction based on Volterra adaptive filter and improved whale optimization algorithm. Eng Appl Artif Intell 2020;87:103323.

[27] Gao WLG, Guirao J, Basavanagoud B, Wu J. Partial multi-dividing ontology learning algorithm. Inf Sci (Ny) 2018;467:35–58. https://doi.org/10.1016/j.ins.2018.07.049.

[28] Gao W, Guirao JLG, Abdel-Aty M, Xi W. An independent set degree condition for fractional critical deleted graphs. Discret Contin Dyn Syst S 2019;12:877–86. https://doi.org/10.3934/dcdss.2019058.

[29] Gao W, Wang W, Dimitrov D, Wang Y. Nano properties analysis via fourth multiplicative ABC indicator calculating. Arab J Chem 2018;11:793–801.

[30] Gao W, Wu H, Siddiqui MK, Baig AQ. Study of biological networks using graph theory. Saudi J Biol Sci 2018;25:1212–9. https://doi.org/10.1016/j.sjbs.2017.11.022.

[31] Chen J, Lu D, Liu W, Fan J, Jiang D, Yi L, et al. Stability study and optimization design of small-spacing two-well (SSTW) salt caverns for natural gas storages. J Energy Storage 2020;27:101131https://doi.org/10.1016/j.est.2019.101131.

[32] Fan J, Jiang D, Liu W, Wu F, Chen J, Daemen JJ. Discontinuous fatigue of salt rock with low-stress intervals. Int J Rock Mech Sci 2019;115:77–86.

[33] Zhang Z, Jiang D, Liu W, Chen J, Li E, Fan J, et al. Study on the mechanism of roof collapse and leakage of horizontal cavern in thinly bedded salt rocks. Environ Earth Sci 2019;78:292.

[34] Weibiao Q, Bingfan L, Zhangyang K. Differential Scanning Calorimetry and Electrochemical Tests for the Analysis of Delamination of 3PE Coatings. Int J Electrochem Sci 2019;14:7389–400. https://doi.org/10.20964/2019.08.05.

[35] Karatepe E, Boztepe M, Colak M. Neural network based solar cell model. Energy Convers Manage 2006;47:1159–78. https://doi.org/10.1016/j.enconman.2005.07.007.

[36] Bonanno F, Capizzi G, Graditi G, Napoli C, Tina GM. A radial basis function neural network based approach for the electrical characteristics estimation of a photovoltaic module. Appl Energy 2012;97:956–61. https://doi.org/10.1016/j.apenergy.2011.12.085.

[37] Khanna V, Das BK, Bisht D, Vandana Singh PK. A three diode model for industrial solar cells and estimation of solar cell parameters using PSO algorithm. Renew. Energy 2015;78:105–13. https://doi.org/10.1016/j.renene.2014.12.072.

[38] Jamadi M, Merrikh-Bayat F, Bigdeli M. Very accurate parameter estimation of single- and double-diode solar cell models using a modified artificial bee colony algorithm. Int J Energy Environ Eng 2016;7:13–25. https://doi.org/10.1007/s40095-015-0198-5.

[39] Ishaque K, Salam Z, Mekhilef S, Shamsudin A. Parameter extraction of solar photovoltaic modules using penalty-based differential evolution. Appl Energy 2012;99:297–308. https://doi.org/10.1016/j.apenergy.2012.05.017.

[40] Jiang LL, Maskell DL, Patra JC. Parameter estimation of solar cells and modules using an improved adaptive differential evolution algorithm. Appl Energy 2013;112:185–93. https://doi.org/10.1016/j.apenergy.2013.06.004.

[41] Gong W, Cai Z. Parameter extraction of solar cell models using repaired adaptive differential evolution. Sol Energy 2013;94:209–20. https://doi.org/10.1016/j.solener.2013.05.007.

[42] Mirjalili S, Gandomi AH, Zahra S, Saremi S. Salp Swarm Algorithm : A bio-inspired optimizer for engineering design problems. Adv Eng Softw 2017:1–29. https://doi.org/10.1016/j.advengsoft.2017.07.002.

[43] Arora S, Singh S. Butterfly optimization algorithm : a novel approach for global optimization. Soft Comput 2018. https://doi.org/10.1007/s00500-018-3102-4.

[44] Ma J, Ting TO, Man KL, Zhang N, Guan S-U, Wong PWH. Parameter estimation of photovoltaic models via cuckoo search. J Appl Math 2013;2013:1–8. https://doi.org/10.1155/2013/362619.

[45] Louzazni M, Khouya A, Amechnoue K, Gandelli A, Mussetta M, Crăciunescu A. Metaheuristic algorithm for photovoltaic parameters: comparative study and prediction with a firefly algorithm. Appl Sci 2018;8:339. https://doi.org/10.3390/app8030339.

[46] Louzazni M, Khouya A, Amechnoue K. A firefly algorithm approach for determining the parameters characteristics of solar cell. Leonardo Electron J Pract Technol 2017:235–50.

[47] Babu TS, Ram JP, Sangeetha K, Laudani A, Rajasekar N. Parameter extraction of two diode solar PV model using Fireworks algorithm. Sol Energy 2016;140:265–76. https://doi.org/10.1016/j.solener.2016.10.044.

[48] Alam DF, Yousri DA, Eteiba MB. Flower Pollination Algorithm based solar PV parameter estimation. Energy Convers Manage 2015;101:410–22. https://doi.org/10.1016/j.enconman.2015.05.074.

[49] Birbil ŞI, Fang SC. An electromagnetism-likemechanism for global optimization. J Glob Optim 2003;25:263–82. https://doi.org/10.1023/A:1022452626305.

[50] Allam D, Yousri DA, Eteiba MB. Parameters extraction of the three diode model for the multi-crystalline solar cell/module using Moth-Flame Optimization Algorithm. Energy Convers Manage 2016;123:535–48. https://doi.org/10.1016/j.enconman.2016.06.052.

[51] Xiong G, Zhang J, Shi D, He Y. Parameter extraction of solar photovoltaic models using an improved whale optimization algorithm. Energy Convers Manage 2018;174:388–405. https://doi.org/10.1016/j.enconman.2018.08.053.

[52] Ali EE, El-Hameed MA, El-Fergany AA, El-Arini MM. Parameter extraction of photovoltaic generating units using multi-verse optimizer. Sustain Energy Technol Assess 2016;17:68–76. https://doi.org/10.1016/j.seta.2016.08.004.

[53] Kler D, Sharma P, Banerjee A, Rana KPS, Kumar V. PV cell and module efficient parameters estimation using Evaporation Rate based Water Cycle Algorithm. Swarm Evol Comput 2017;35:93–110. https://doi.org/10.1016/j.swevo.2017.02.005.

[54] Gnetchejo PJ, Ndjakomo Essiane S, Ele P, Wamkeue R, Mbadjoun Wapet D, Perabi Ngoffe S. Important notes on parameter estimation of solar photovoltaic cell. Energy Convers Manage 2019;197:111870https://doi.org/10.1016/j.enconman.2019.111870.

[55] Aljarah I, Mafarja M, Heidari AA, Faris H, Mirjalili S. Clustering analysis using a novel locality-informed grey wolf-inspired clustering approach. Knowl Inf Syst 2019. https://doi.org/10.1007/s10115-019-01358-x.

[56] Faris H, Alam A-Z, Heidari AA, Aljarah I, Mafarja M, Hassonah MA, et al. An intelligent system for spam detection and identification of the most relevant features based on evolutionary Random Weight Networks. Inf Fusion 2019;48:67–83.

[57] Faris H, Mafarja MM, Heidari AA, Aljarah I, Alam A-Z, Mirjalili S, et al. An efficient binary Salp Swarm Algorithm with crossover scheme for feature selection problems. Knowl Based Syst 2018;154:43–67.

[58] Mafarja M, Aljarah I, Heidari AA, Faris H, Fournier-Viger P, Li X, et al. Binary dragonfly optimization for feature selection using time-varying transfer functions. Knowl Based Syst 2018;161:185–204. https://doi.org/10.1016/j.knosys.2018.08.003.

[59] Faris H, Heidari AA, Al-Zoubi AM, Mafarja M, Aljarah I, Eshtay M, et al. Time-varying hierarchical chains of salps with random weight networks for feature selection. Expert Syst Appl 2019;140:112898https://doi.org/10.1016/j.eswa.2019.112898.

[60] Heidari AA, Aljarah I, Faris H, Chen H, Luo J, Mirjalili S. An enhanced associative learning-based exploratory whale optimizer for global optimization. Neural Comput Appl 2019. https://doi.org/10.1007/s00521-019-04015-0.

[61] Chen X, Yu K. Hybridizing cuckoo search algorithm with biogeography-based optimization for estimating photovoltaic model parameters. Sol Energy 2019;180:192–206. https://doi.org/10.1016/j.solener.2019.01.025.

[62] Abbassi R, Abbassi A, Asghar A, Mirjalili S. An efficient salp swarm-inspired algorithm for parameters identification of photovoltaic cell models. Energy Convers Manage 2019;179:362–72. https://doi.org/10.1016/j.enconman.2018.10.069.

[63] Rezaee Jordehi A. Enhanced leader particle swarm optimisation (ELPSO): An efficient algorithm for parameter estimation of photovoltaic (PV) cells and modules. Sol Energy 2018;159:78–87. https://doi.org/10.1016/j.solener.2017.10.063.

[64] Yu K, Liang JJ, Qu BY, Cheng Z, Wang H. Multiple learning backtracking search algorithm for estimating parameters of photovoltaic models. Appl Energy 2018;226:408–22. https://doi.org/10.1016/j.apenergy.2018.06.010.

[65] Chin VJ, Salam Z, Ishaque K. An accurate modelling of the two-diode model of PV module using a hybrid solution based on differential evolution. Energy Convers Manage 2016;124:42–50. https://doi.org/10.1016/j.enconman.2016.06.076.

[66] Yousri D, Allam D, Eteiba MB, Suganthan PN. Static and dynamic photovoltaic models' parameters identification using Chaotic Heterogeneous Comprehensive Learning Particle Swarm Optimizer variants. Energy Convers Manage 2019;182:546–63. https://doi.org/10.1016/j.enconman.2018.12.022.

[67] Kler D, Goswami Y, Rana KPS, Kumar V. A novel approach to parameter estimation of photovoltaic systems using hybridized optimizer. Energy Convers Manage 2019;187:486–511. https://doi.org/10.1016/j.enconman.2019.01.102.

[68] Del Ser J, Osaba E, Molina D, Yang X, Salcedo-sanz S, Camacho D, et al. Bio-inspired computation: Where we stand and what's next. Swarm Evol Comput Base Data 2019. https://doi.org/10.1016/j.swevo.2019.04.008.

[69] Wolpert DHG, Macready WG. No free lunch theorems for optimization. IEEE Trans Evol Comput 1997;1:67–82.

[70] Chen H, Jiao S, Wang M, Heidari AA, Zhao X. Parameters identification of photovoltaic cells and modules using diversification-enriched Harris hawks optimization with chaotic drifts. J Clean Prod 2019;118778. https://doi.org/10.1016/j.jclepro.2019.118778.

[71] Ridha HM, Gomes C, Hizam H. Estimation of photovoltaic module model's parameters using an improved electromagnetic-like algorithm. Neural Comput Appl 2020. https://doi.org/10.1007/s00521-020-04714-z.

[72] Chen H, Jiao S, Heidari AA, Wang M, Chen X, Zhao X. An opposition-based sine cosine approach with local search for parameter estimation of photovoltaic models. Energy Convers Manage 2019;195:927–42. https://doi.org/10.1016/j.enconman.2019.05.057.

[73] Villalva MG, Gazoli JR, Filho ER. Comprehensive approach to modeling and simulation of photovoltaic arrays. IEEE Trans Power Electron 2009;24:1198–208. https://doi.org/10.1109/tpel.2009.2013862.

[74] Yahya-khotbehsara A, Shahhoseini A. A fast modeling of the double-diode model for PV modules using combined analytical and numerical approach. Sol Energy 2018;162:403–9. https://doi.org/10.1016/j.solener.2018.01.047.

[75] Heidari AA, Mirjalili S, Faris H, Aljarah I, Mafarja M, Chen H. Harris hawks optimization: algorithm and applications. Fut Gener Comput Syst 2019;97:849–72. https://doi.org/10.1016/j.future.2019.02.028.

[76] Golilarz NA, Gao H, Demirel H, Member S. Satellite image de-noising with Harris Hawks Meta heuristic optimization algorithm and improved adaptive generalized Gaussian distribution threshold function. IEEE Access 2019;1. https://doi.org/10.1109/ACCESS.2019.2914101.

[77] Assistant SM. Harris hawks optimization for solving optimum load dispatch problem in power system. Int J Eng Res Technol 2019;8:962–8.

[78] Thaher T, Heidari AA, Mafarja M, Dong JS, Mirjalili S. Binary Harris hawks optimizer for high-dimensional, low sample size feature selection. In: Mirjalili S, Faris H, Aljarah I, editors. Evol. Mach. Learn. Tech. Algorithms Appl. Singapore: Springer Singapore; 2020. p. 251–72. https://doi.org/10.1007/978-981-32-9990-0_12.

[79] Bednarz JC. Cooperative hunting in harris' hawks (parabuteo unicinctus). Science 1988;239:1525–7.
[80] Viswanathan GM, Afanasyev V, Buldyrev SV, Murphy EJ, Prince PA, Stanley HE. Lévy flight search patterns of wandering albatrosses. Nature 1996;381:413–5. https://doi.org/10.1038/381413a0.
[81] Flower Yang X-S. pollination algorithm (FPA). Nature-Inspired Optim Algorithms Elsevier; 2014. p. 155–73. https://doi.org/10.1016/B978-0-12-416743-8.00011-7.
[82] Reddy PDP, Reddy VCV, Manohar TG. Application of flower pollination algorithm for optimal placement and sizing of distributed generation in Distribution systems. J Electr Syst Inf Technol 2016;3:14–22. https://doi.org/10.1016/j.jesit.2015.10.002.
[83] Croes GA. A method for solving traveling-saleman problems. Oper Res 1958;6:791–812. https://doi.org/10.4103/0019-557X.75737.
[84] Das S, Mullick SS, Suganthan PN. Recent advances in differential evolution-An updated survey. Swarm Evol Comput 2016;27:1–30. https://doi.org/10.1016/j.swevo.2016.01.004.
[85] Muhsen DH, Ghazali AB, Khatib T, Abed IA. Parameters extraction of double diode photovoltaic module's model based on hybrid evolutionary algorithm. Energy Convers Manage 2015. https://doi.org/10.1016/j.enconman.2015.08.023.